Energy Proceedings
Vol 41, 2024

ISSN 2004-2965

Towards Sustainable Fertilizer Production: Cost Comparison of Flexible and Continuous Electrolytic Ammonia Production

Stefano Mingolla[1*], Kevin Rouwenhorst[2], Paolo Gabrielli[3], Giovanni Sansavini[3], Magdalena M. Klemun[4,5], Zhongming Lu[1*]

1 Division of Environment and Sustainability, The Hong Kong University of Science and Technology, Clear Water Bay, Kowloon, Hong Kong SAR (Corresponding Author)

2 Ammonia Energy Association, 44927 George Washington Blvd, Ste 265 Ashburn, VA 20147, USA

3 Reliability and Risk Engineering, Institute of Energy and Process Engineering, ETH Zürich, Zurich 8092, Switzerland

4 Energy Institute, The Hong Kong University of Science and Technology, Hong Kong SAR

5 Division of Public Policy, The Hong Kong University of Science and Technology, Clear Water Bay, Kowloon, Hong Kong SAR

ABSTRACT

Ammonia production contributes 1% of global carbon emissions due to energy-intensive hydrogen synthesis. To mitigate this, renewable-powered water electrolysis is a promising solution. While numerous studies have explored the use of hydrogen storage and grid backup to align renewable energy sources with the continuous operation of the HB process, recent industry efforts focused on increasing plant flexibility, adjusting the production to intermittent power inputs. In this study, we model and optimize two plant configurations—continuous and flexible. The aim is to determine the conditions under which flexible production reduces costs. Our results show that renewable resource availability has a significantly greater impact on LCOA than plant configuration. For the same configuration, LCOA differs by a factor of two across regions with low and high-capacity factors. Continuous plants have lower LCOA in solar-dominated regions (-13%). In contrast, flexible plants are more cost-effective in wind-rich regions (-12%) or ones with high-capacity factors for renewable production (-11%) due to their ability to maintain the minimum load with less reliance on batteries or grid imports. The lowest LCOA is 372 EUR/ton NH_3 in high-capacity regions, followed by wind-dominated areas (389 EUR/ton NH_3), both with flexible configurations.

Keywords: low-carbon hydrogen, electrolytic ammonia, flexible production, chemical industry decarbonization, energy systems modeling, sustainable fertilizers

NOMENCLATURE

Abbreviations	
ALK	Alkaline Electrolyzer
ASU	Air Separator Unit
BESS	Battery Energy Storage Systems
CF	Capacity Factor
HB	Haber-Bosch
LCOA	Levelized Cost Of Ammonia
LIB	Li-ion Batteries
PV	Photovoltaics
SMR	Steam Methane Reforming
WT	Wind Turbines
Indices	
l	Year
t	Time-step (hour)
Sets	
$\mathcal{J}$	Energy carriers
$\mathcal{K}$	Technologies
Energy carrier	
E	Electricity
$\mathrm{H_2}$	Hydrogen
$\mathrm{N_2}$	Nitrogen
$\mathrm{NH_3}$	Ammonia
Parameters	
c	Technology Investment Cost
D	Plant Output
p	Energy Price
s	Solar Energy
v	Technology Operation & Maintenance
w	Wind Energy
η	Technology Performance
γ	Grid Energy Carbon Footprint
ω	Renewables Capacity Factor
Variables	
b	Technology Selection

This is a paper for 15th International Conference on Applied Energy (ICAE2023), Dec. 3-7, 2023, Doha, Qatar.

M	Imported Energy
P	Technology Size
U	Input Energy
V	Output Energy
y	ON/OFF Scheduling

1. INTRODUCTION

Ammonia (NH_3) production is responsible for approximately 1% of the world's carbon dioxide equivalent (CO_2e) emissions, with most of this carbon footprint attributed to the energy-intensive hydrogen production process, primarily derived from methane via SMR [1,2]. The volatility of natural gas prices and increasing concern over climate change have sparked interest in alternative ammonia production methods [3]. Electrolytic ammonia, which uses renewably powered water electrolysis to generate hydrogen and subsequently combines it with nitrogen for synthesis in the HB loop, is an alternative [4,5]. This method holds promising potential to cut the industry's carbon emissions significantly. However, one critical challenge lies in aligning the constant operational conditions required by the HB process with the intermittent nature of renewable energy.

To investigate the potential of flexible ammonia production for decarbonizing the industry, we develop a modeling framework and optimization approach for large-scale, semi-islanded electrolytic ammonia plants. We compare different plant layouts, including continuous and flexible configurations. The optimization uses mixed-integer linear programming (MILP) techniques to optimize the plant's design and operations. Our key research question is: Under which renewable conditions do flexible plants have lower LCOA than continuous plants?

Our study aims to provide a more comprehensive understanding of the potential benefits and challenges associated with flexible ammonia production, which will aid future efforts to decarbonize the ammonia industry and inform policy decisions.

2. MATERIAL AND METHODS

To address our research questions, we model and subsequently optimize two distinct ammonia plant setups, namely (i) continuous plant and (ii) flexible plant, as shown in Fig. 1. The objective function is to minimize the lifetime system cost (eq. 1), while the decision variables are the design and operation of the ammonia plants under different input parameter assumptions.

$$min\ z_{cost} = \sum_{k\in\mathcal{K}} I_k + \sum_{k\in\mathcal{K}} v_k\, I_k + \sum_{l=1}^{L}\sum_{t=0}^{T} p_{\mathrm{E}}(M_{\mathrm{E},t}) \qquad \text{eq. 1}$$

Where $\mathrm{z}_{\mathrm{cost}}$ represents the total lifetime cost of the electrolytic ammonia plant minimized by our model, consisting of the sum of capital cost I_k operation and maintenance cost (O&M) $v_k I_k$, and grid power purchase $p_{\mathrm{E}}(M_{\mathrm{E},t})$.

$$\mathrm{LCOA} = \frac{\mathrm{z}_{\mathrm{cost}}}{\sum_{l=1}^{L}\sum_{t=1}^{T} D_{\mathrm{NH3},t}^{h}} \qquad \text{eq. 2}$$

From eq. 2 we derive the LCOA. We assume that the total amount of ammonia produced $\sum_{l=1}^{L}\sum_{t=1}^{T} D_{\mathrm{NH3},t}^{h}$ ($D_{\mathrm{NH3},t}^{h}$ is the hourly NH_3 output of the plant), remains consistent regardless of the chosen plant layout or assumptions regarding input parameters. This allows for a meaningful comparison of LCOA across diverse scenarios, enabling a comprehensive assessment of the economic viability of ammonia production.

We assume to install all the components in 2025 and start operations on January 1, 2026, until December 31, 2050.

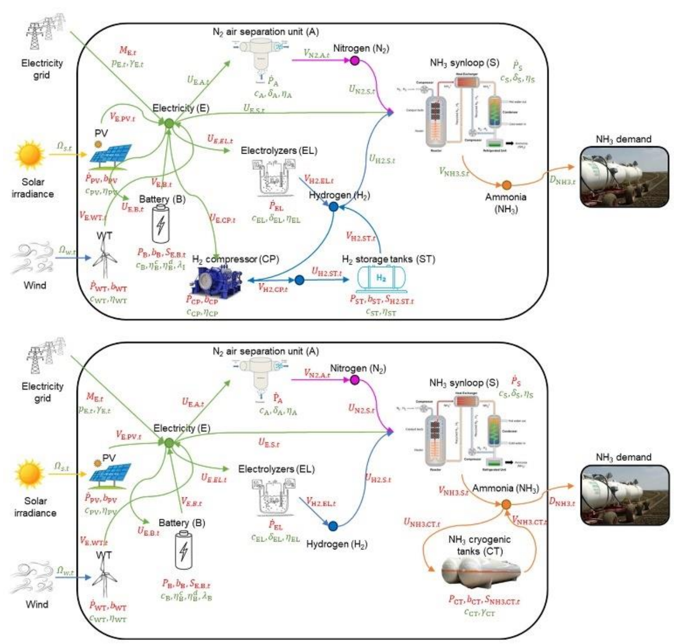

Fig. 1: Electrolytic ammonia plant subsystems. (a) continuous plant; (b) flexible plant. Variables in red indicate the decision variables of the model, while variables in green are input parameters for the optimization model.

2.1 Electrolytic Ammonia Plants Subsystems

Despite advancements in process technology, the fundamental chemistry of the HB process has remained largely unchanged since its original development. While different pathways exist for producing the necessary feed hydrogen, such as SMR in conventional plants and electrolytic hydrogen in our proposed study, the core components of the plant remain largely unchanged.

2.1.1 Renewable Resources

We utilize historical capacity factors derived from the Copernicus Climate Change Service (C3S) dataset [6]. The capacity factor is a crucial metric in energy studies, representing the ratio of the actual generation to the installed capacity. The C3S dataset provides historical capacity factors from 1979 to the present in Europe. We adopt a representative approach due to computational constraints associated with simulating all potential climate conditions and considering the extensive temporal resolution of the data (hourly).

First, we calculate the mean annual capacity factor $\overline{\omega}_{R,i,j}$ for each region i and year j for both solar and wind energy sources ω_R ($R: \{solar: s; wind: w\}$) according to eq. 3. Next, we identify regions with the highest, median, and lowest mean annual capacity factors for wind and solar installations to create five distinct "synthetic regions" representing extreme weather scenarios (Fig. 2). These include (i) wind-dominated, (ii) solar-dominated, (iii) low-capacity, (iv) median-capacity, and (v) high-capacity (both solar and wind).

$$\overline{\omega}_{R,i,j} = \frac{\sum_{t=0}^{T} \omega_{R,i,j,t}}{T} \qquad \text{eq. 3}$$

The high-capacity region combines the highest solar and wind capacity factors. The median-capacity region uses the median values for solar and wind capacity factors. The solar-dominated region has the highest solar capacity factor and the lowest wind capacity factor. The wind-dominated region has the lowest solar capacity factor and the highest wind capacity factor. Data from regions at the 25th percentile for solar and wind capacity factors are used for the low-capacity region.

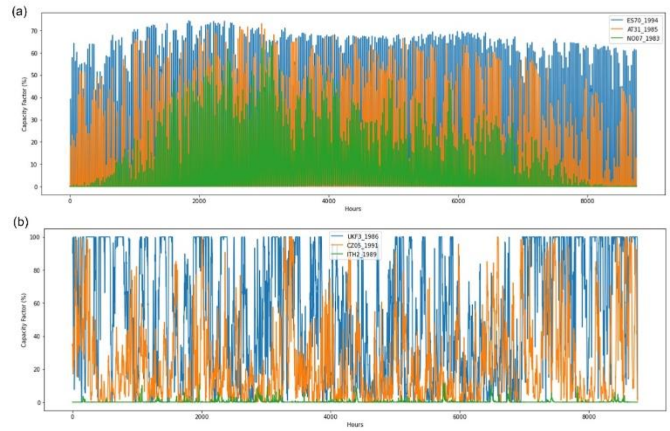

Fig. 2: Highest, median, and lowest mean annual capacity factors across EU NUTS-2 regions from 1979 to 2022. (a) 19%; 12%; 7% for solar capacity factor; (b) 57%; 23%; 1% for wind capacity factor.

2.1.2 Photovoltaics and Wind Turbines Installations

To maximize the utilization of local renewable resources and optimize ammonia production, we assume the installation of utility-scale PV and onshore WT. We obtain cost and performance data for these renewable energy systems from the IRENA database, widely recognized as one of the most comprehensive sources of information on renewable projects worldwide [7]. We consider the global-weighted average total installed cost of PV and WT provided by IRENA as reference value for our analysis (668,182 EUR/MW and 1,445,455 EUR/MW as the estimated installation cost for solar PV and WT, respectively).

2.1.3 Grid Electricity Costs and Emissions

Grid electricity can complement renewable sources by extending operational hours and reducing the need for larger installed capacity and associated costs [8–10]. Hence, we propose a semi-islanded configuration for the ammonia plants, allowing the importation of grid electricity as a backup. The optimization model determines the optimal amount of imported electricity, denoted as $M_{\mathrm{E},t}$, for each hour.

Nevertheless, the reliance on grid electricity results in carbon emissions, especially in regions where the electricity mix heavily relies on fossil fuels [8,10]. The carbon footprint of electrolytic ammonia remains a contentious issue. Previous studies [11] suggested that an emission limit of 1 kg of CO_2e per kg of H_2 is a cost-effective cap for electrolytic hydrogen in ammonia production, and we adopt this benchmark for our current research. This implies we can import grid electricity if the lifetime average emissions of hydrogen do not exceed the 1 kg CO_2e /kg H_2 limit (eq. 4).

$$\sum_{l=0}^{L}\sum_{t=0}^{T}\gamma_{\mathrm{E}}M_{\mathrm{E},t} \leq \varepsilon_{\mathrm{H2}}\left(\sum_{l=0}^{L}\sum_{t=0}^{T}U_{\mathrm{H2,S},t}\right) \quad \text{eq. 4}$$

Where γ_{E} is the carbon intensity of grid electricity in kg CO_2e/kg H_2, while $\varepsilon_{\mathrm{H2}}$ represents the emission threshold implemented. $U_{\mathrm{H2,S},t}$ instead, is the hourly hydrogen input of the ammonia synloop.

To calculate the average carbon intensity of grid electricity, we collect data on the carbon intensity of the electricity mix worldwide from Our World in Data [12]. We assume that all electricity grids will achieve carbon neutrality by 2050, employing a linear reduction approach from the present to 2050. As per this, we use 152 kg CO_2e/MWh.

Regarding electricity prices, we collect historical electricity prices for large-scale industrial users from the International Energy Agency [13,14]. We select the median price of 111.55 EUR/MWh.

2.1.4 Battery Energy Storage Systems

We collect the cost and performance of utility-scale BESS utilizing LIBs from the National Renewable Energy Laboratory's 2023 Annual Technology Baseline [15] (652,808 EUR/MWh). We consider a LIB with a duration of 4 hours and a round trip efficiency of 86% [15], with losses equally distributed between charging and discharging. We also account for a conservative 15-year lifetime for the LIB pack [16].

2.1.5 Electrolyzers

We collect data regarding ALK electrolyzer cost and performances from various sources, including the Hydrohub Innovation Program's extensive literature review conducted in 2022 [17]. This review assessed the costs of large-scale (1-GW) electrolytic-hydrogen production systems. According to their projection, a 50% reduction in electrolyzer system costs is projected between 2020 and 2030. We, therefore, assume a linear cost reduction trend to align with this projection. Since plants are assumed to install all subsystems in 2025, we anticipate a 25% reduction in costs compared to the 2020 data. The total system cost of the electrolyzer is 1,164,774 EUR/MW, while the energy demand is 52 kWh/kg H_2.

2.1.6 Hydrogen Compressors and Storage Tanks

In the continuous plant layout, excess renewable electricity can be utilized to synthesize hydrogen, which can then be stored for balancing periods. However, since ALK electrolyzers typically operate at lower pressures (ranging from atmospheric pressure to 30 bar), mechanical compression becomes essential to achieve the desired pressure of approximately 350 bar, commonly used for hydrogen storage tanks. Therefore, a compression process is employed to elevate the pressure to the required level for efficient storage. The estimated electricity consumption for compressing hydrogen to this pressure is around 2 kWh/kg H_2 [18]. Regarding investment costs, we assume 10,000 EUR/kg H_2/h for the compressor and 455 EUR/kg H_2 for the high-pressure tank based on the study conducted by Ikäheimo et al. [18].

2.1.7 Air Separator Unit

ASUs purify nitrogen (N_2) directly from the air. Cryogenic distillation offers the purest product with the lowest specific energy consumption (0.1 kWh/kg N_2), making it economically advantageous for large-scale electrically driven ammonia production facilities [19].

An inherent limitation of ASUs, particularly cryogenic distillation, is their inability to operate below a minimum load δ_{A} of 50% of the nominal capacity. This minimum load requirement ensures efficient operation, product quality, and system safety.

2.1.8 Ammonia Synloop

The HB ammonia synthesis loop comprises several components: a synthesis reactor, mixing units, compressors, heat exchangers, and an ammonia separation unit. Operating within a pressure range of 150 to 300 bar and temperatures between 350 to 550°C, these conditions are carefully selected to optimize the reaction rate, considering that the yield per single pass typically ranges from 15 to 25%.

One of the main challenges in achieving operational flexibility lies in minimizing load variability within the ammonia synthesis loop. The reactor's characteristics limit dynamic operation, necessitating a continuous supply of hydrogen, nitrogen, and process electricity [20].

As assumed for the ASU, we choose a 50% minimum load δ_{S}.

2.1.9 Cryogenic Storage

Cryogenic tanks are specialized containers designed to store ammonia at cryogenic temperatures, usually below -33°C.

Conventional ammonia plants typically incorporate cryogenic storage tanks with a capacity equivalent to two weeks' worth of ammonia production. However, in the case of a flexible plant layout, we include the possibility of installing supplementary cryogenic storage tanks to serve as a buffer.

2.2 Modeling a Continuous Plant

In the continuous plant layout (Fig. 1a), the ammonia plants operate non-stop, ensuring an uninterrupted ammonia output $V_{\mathrm{NH3,S},t}$ of approximately 42 t NH_3/h (equivalent to 1000 t NH_3/d) (eq. 5). To maintain this constant ammonia output, a continuous supply of hydrogen $U_{\mathrm{H2,S},t}$ is required for the synloop (eq. 6). Several methods can be employed to achieve this sustained hydrogen supply. Firstly, renewable energy sources and grid electricity can be utilized while adhering to emission constraints. If batteries are installed, the stored energy can also contribute to maintaining steady-state plant operations. Moreover, the energy surplus from peak renewable hours can be used to produce a hydrogen surplus, later compressed using dedicated hydrogen compressors and stored in high-pressure tanks.

$$V_{\mathrm{NH3,S},t} = D_{\mathrm{NH3}}^{h},\ \forall\, t \in \{0, \dots, T\} \qquad \text{eq. 5}$$

$$U_{\mathrm{H2,S},t} = V_{\mathrm{H2,EL},t} - U_{\mathrm{H2,ST},t} + V_{\mathrm{H2,ST},t},\ \forall\, t \in \{0, \dots, T\} \qquad \text{eq. 6}$$

Where D_{NH3}^{h} is a constant representing the amount of ammonia that must be produced each hour of the year; $V_{\mathrm{H2,EL}.t}$ is the hourly hydrogen output the electrolyzer; $U_{\mathrm{H2,ST},t}$ is the volume of hydrogen entering as input for the storage tank, and $V_{\mathrm{H2,ST},t}$ is the output hydrogen of the storage tank in hour t.

2.3 Modeling a Flexible Plant

There is no unique definition of flexibility since its interpretation can vary depending on the context and perspective. In our paper, flexibility is the capacity to adjust output throughout the day, seamlessly following the input energy from renewable sources. The greater the ability to track the renewables, the greater the flexibility. The plant's flexibility level is tied to the least flexible technology's degree of flexibility, implying that any constraints on such technology's output or load capacity will limit all other systems.

The annual of ammonia $\mathrm{D}_{\mathrm{NH3}}^{\mathrm{y}}$ of flexible plants remains the same as the continuous plant layout (365,000 t NH_3/y), but the plant operates dynamically to produce ammonia during periods of high renewable energy supply and eventually store it in additional ammonia storage tanks for periods of low renewable energy supply (Fig. 1b). This eliminates the need for hydrogen compressors and storage but may eventually require additional ammonia storage capacity, which we model and optimize in our analysis. Unlike the continuous plant, in the flexible plant layout, we also optimize the hourly output of ammonia $D_{\mathrm{NH3},t}^{h}$ as a decision variable (eq. 7). The flexibility of the plant operation enables it to adjust ammonia production in response to changing renewable energy supply and demand and potentially reduce overall LCOA by optimizing production.

$$\sum_{t=0}^{T} D_{\mathrm{NH3},t}^{h} = D_{\mathrm{NH3}}^{y} \qquad \text{eq. 7}$$

Where the hourly output of ammonia $D_{\mathrm{NH3},t}^{h}$ is equal to the output of the ammonia synloop $V_{\mathrm{NH3,S},t}$, minus the ammonia entering the cryogenic storage $U_{\mathrm{NH3,CT},t}$, plus the output of ammonia from the storage $V_{\mathrm{NH3,CT},t}$ (eq. 8).

$$D_{\mathrm{NH3},t}^{h} = V_{\mathrm{NH3,S},t} - U_{\mathrm{NH3,CT},t} + V_{\mathrm{NH3,CT},t},\ \forall\, t \in \{0, \dots, T\} \qquad \text{eq. 8}$$

3. RESULTS

The LCOA for continuous and flexible electrolytic ammonia plants across the five representative synthetic regions is presented in Fig. 3.

Regardless of the type of plant, local renewable energy availability significantly affects the optimal design and operation of the plant, which, in turn, influences the LCOA. The highest LCOA is in low-capacity regions with a continuous configuration (1070 EUR/t NH_3), while the lowest LCOA is in high-capacity regions with flexible plant layout (372 EUR/t NH_3), closely followed by wind-dominated regions (389 EUR/t NH_3).

Plants in regions dominated by wind energy show lower costs, primarily due to the reduced need for extensive renewable energy infrastructure and less reliance on battery storage or grid backup, as demonstrated by other research [21]. This is because solar power is typically concentrated within limited daily hours, irrespective of the solar energy's intensity during those hours. On the other hand, wind energy is more evenly distributed throughout the day and night, making it easier to ensure extended operational hours for the plant when it primarily depends on renewables (semi-islanded).

Interestingly, plants in areas characterized by moderate and balanced solar and wind resources demonstrate costs similar to those seen in solar-dominated regions. However, the plant design in these regions differs significantly, with hybrid solar and wind installations favored in median-capacity regions.

The second key finding is that flexible plants present lower costs in wind-dominated regions and regions with high renewable potential (both solar and wind), showing a 10% cost reduction compared to continuous plants in the same regions. In contrast, a semi-flexible layout incurs significantly higher costs than continuous plants in solar-dominated regions (+13% LCOA). This reiterates the challenge of maintaining the minimum load required by the ASU and ammonia synthesis loop when dependent on intermittent resources. Therefore, substantial battery installations are required in regions with limited wind resources, leading to a significant cost increase. LCOA in median-capacity and low-capacity regions are similar for both continuous and semi-flexible plants.

4. DISCUSSION AND CONCLUSIONS

In this study, we develop a modeling framework and optimization approach for large-scale, semi-islanded electrolytic ammonia plants. We compare different plant layouts, including continuous and flexible configurations.

Our findings confirm that the renewable potential of a region plays a significant role in determining LCOA and carbon emissions. Regions with abundant renewable resources require smaller renewable generation infrastructures, resulting in a lower cost per unit produced due to increased output per unit of installed capacity. Enhanced renewable capacity factors also diminish grid imports to balance power shortages, reducing operational emissions.

In terms of plant types, continuous plants yield a lower LCOA in solar-dominated regions. In contrast, flexible configurations are more cost-effective in wind-dominated areas and regions with high-capacity factors. The challenge lies in maintaining the minimum load of ASU and ammonia synloop at night when predominantly relying on solar power. Solar energy, which sees peaks during the day, necessitates substantial battery storage or grid support, particularly when the plant subsystems' minimum load cannot accommodate low-capacity operations. Therefore, using a continuous layout where hydrogen surplus produced during peak renewable hours can be stored for nighttime usage might be advantageous. The opposite is true for wind-dominated regions that benefit from more consistent power availability and can benefit from a flexible layout.

While our study sheds light on the costs of different plant types in specific regions, it is important to note that the observed differences in LCOA are relatively small. Therefore, it is crucial to further investigate and test the robustness of these findings. Moreover, future research should also focus on exploring additional degrees of flexibility in plant configurations. Technology licensors are in fact focusing on alternative configurations of ammonia synthesis loops and ASU that have lower minimum load capacity and faster ramp rates. This will enable better adaptation to variable renewable energy sources and ensure efficient operation even during periods of low power generation. By delving into these aspects, future research can provide a more comprehensive understanding of the industry's potential for development and pave the way for advancements in the field of renewable ammonia production.

Our findings provide valuable insights for plant operators, industry stakeholders, and policymakers, guiding them in formulating effective strategies for decarbonizing ammonia production.

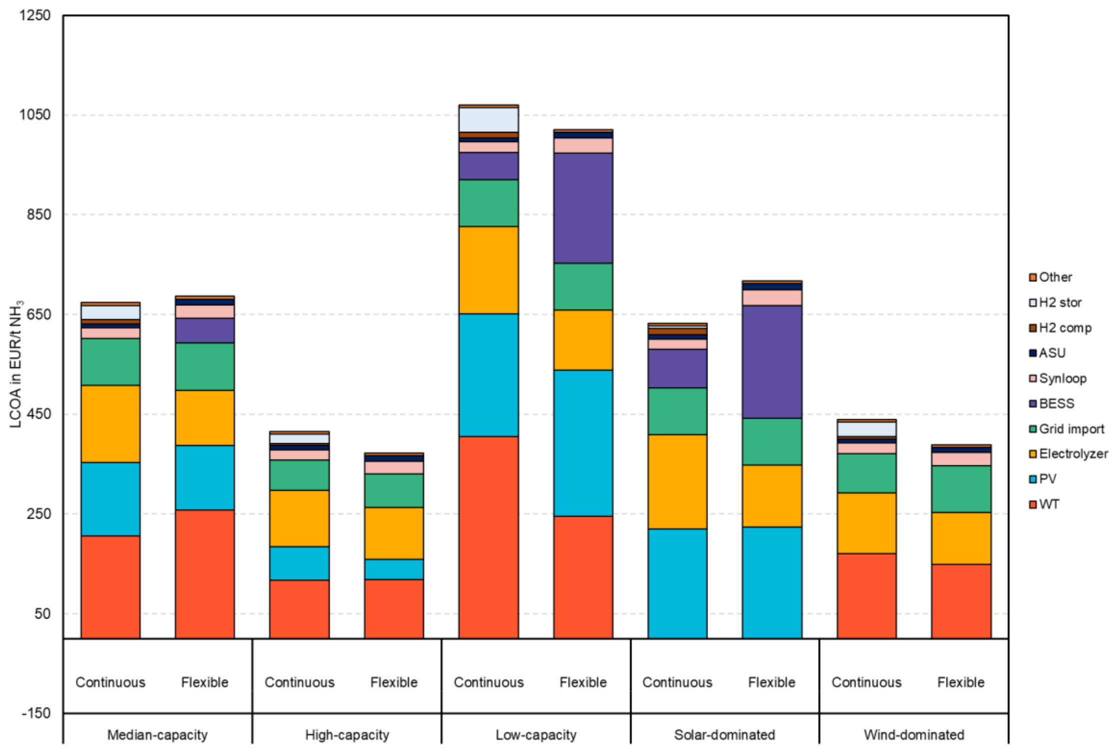

Fig. 3: LCOA for continuous and flexible electrolytic ammonia plants in different representative synthetic regions.

ACKNOWLEDGEMENT

The work was supported by the Hong Kong Research Grant Council (26201721) and start-up support from the Hong Kong University of Science and Technology. S.M. gratefully acknowledges the support from the Research Grants Council of Hong Kong through the Hong Kong Ph.D. Fellowship Scheme (HKPFS).

DECLARATION OF INTEREST STATEMENT

The authors declare that they have no known competing financial interests or personal relationships that could have appeared to influence the work reported in this paper. All authors read and approved the final manuscript.

REFERENCE

[1] IRENA. Innovation Outlook - Renewable Ammonia. 2022.

[2] Rogers M, Delasalle F, Speelman E, Hoffman J, Shah T, Wuellenweber J, et al. Making Net-Zero Ammonia Possible - An industry-backed, 1.5C-aligned transition strategy. 2022.

[3] Saygin D, Blanco H, Boshell F, Cordonnier J, Rouwenhorst K, Lathwal P, et al. Ammonia Production from Clean Hydrogen and the Implications for Global Natural Gas Demand. Sustainability 2023;15:1623. https://doi.org/10.3390/su15021623.

[4] Valera-Medina A, Bãnares-Alcántara R, Rouwenhorst KHR, Krzywda PM, Benes NE, Mul G, et al. Techno-Economic Challenges of Green Ammonia as an Energy Vector - Chapter 4. Elsevier; 2020. https://doi.org/10.1016/B978-0-12-820560-0.00001-1.

[5] Smith C, Hill AK, Torrente-Murciano L. Current and future role of Haber–Bosch ammonia in a carbon-free energy landscape. Energy Environ Sci 2020;13:331–44. https://doi.org/10.1039/C9EE02873K.

[6] Copernicus Climate Change Service. Climate and energy indicators for Europe from 1979 to present derived from reanalysis. 2020. https://doi.org/10.24381/cds.4bd77450.

[7] IRENA. Renewable Power Generation Costs in 2020. 2021.

[8] Salmon N, Bañares-Alcántara R. Impact of grid connectivity on cost and location of green ammonia production: Australia as a case study. Energy Environ Sci 2021;14:6655–71. https://doi.org/10.1039/D1EE02582A.

[9] Campion N, Nami H, Swisher PR, Vang Hendriksen P, Münster M. Techno-economic assessment of green ammonia production with different wind and solar potentials. Renewable and Sustainable Energy Reviews 2023;173. https://doi.org/10.1016/j.rser.2022.113057.

[10] Terlouw T, Bauer C, McKenna R, Mazzotti M. Large-scale hydrogen production via water electrolysis: a techno-economic and environmental assessment. Energy Environ Sci 2022;15:3583–602. https://doi.org/10.1039/d2ee01023b.

[11] Hydrogen Science Coalition. Clean Hydrogen Definition. 2022.

[12] Our World in Data. Carbon intensity of electricity, 2022 2022. https://ourworldindata.org/grapher/carbon-intensity-electricity?time=2022 (accessed August 29, 2023).

[13] IEA. Industry end-user electricity prices in selected OECD countries, 2019 2020. https://www.iea.org/data-and-statistics/charts/industry-end-user-electricity-prices-in-selected-oecd-countries-2019 (accessed August 29, 2023).

[14] IEA. Electricity Market Report. 2020.

[15] NREL. Utility-Scale Battery Storage | Electricity | 2023 2023. https://atb.nrel.gov/electricity/2023/utility-scale_battery_storage (accessed August 29, 2023).

[16] Kebede AA, Kalogiannis T, Van Mierlo J, Berecibar M. A comprehensive review of stationary energy storage devices for large scale renewable energy sources grid integration. Renewable and Sustainable Energy Reviews 2022;159:112213. https://doi.org/10.1016/J.RSER.2022.112213.

[17] Hydrohub Innovation Program. A One-GigaWatt Green-Hydrogen Plant - Advanced Design and Total Installed-Capital Costs. 2022.

[18] Ikäheimo J, Kiviluoma J, Weiss R, Holttinen H. Power-to-ammonia in future North European 100 % renewable power and heat system. Int J Hydrogen Energy 2018;43:17295–308. https://doi.org/10.1016/J.IJHYDENE.2018.06.121.

[19] Morgan E, Manwell J, McGowan J. Wind-powered ammonia fuel production for remote islands: A case study. Renew Energy 2014;72:51–61. https://doi.org/10.1016/J.RENENE.2014.06.034.

[20] Wang C, Walsh SDC, Longden T, Palmer G, Lutalo I, Dargaville R. Optimising renewable generation configurations of off-grid green ammonia production systems considering Haber-Bosch flexibility. Energy Convers Manag 2023;280:116790. https://doi.org/10.1016/J.ENCONMAN.2023.116790.

[21] Armijo J, Philibert C. Flexible production of green hydrogen and ammonia from variable solar and wind energy: Case study of Chile and Argentina. Int J Hydrogen Energy 2020;45:1541–58. https://doi.org/10.1016/j.ijhydene.2019.11.028.